

# Feasibility study of magnetic fluid support and lubrication behaviors on micro magnet arrays

Jingbing Li, Qingwen Dai, Wei Huang<sup>\*</sup>, Xiaolei Wang

National Key Laboratory of Science and Technology on Helicopter Transmission, Nanjing University of Aeronautics & Astronautics, Nanjing, 210016, China

## ARTICLE INFO

### Keywords:

Magnetic fluid  
Support  
Lubrication  
Magnetic field

## ABSTRACT

Magnetic fluid (MF) is a kind of magnetically controlled colloid, which may serve as an active medium in support and lubrication systems. This paper presents a design of micro magnet arrays for MF lubrication associated with fluid/gas supports. By using electrochemical machining and electroplating techniques, thick micro magnet arrays with sheet and ring cells were fabricated in 316 stainless steel substrate. The support and lubrication behaviors of MF absorbed on the magnet arrays were tested and compared. Results confirm that MF fixed on the magnet arrays possesses a certain load carrying capacity. Due to the supporting capacity, low friction coefficient of 0.003 can be achieved. Under high load condition, the magnetic surfaces only show friction reduction at the higher speeds.

## 1. Introduction

The attempt to decrease friction between sliding surfaces is an eternal pursuit of human beings. Fluid film lubrication is one of the ideal states, through which the rubbing surfaces can be totally isolated by a squeezed lubricant film. Friction is only originated from the shearing of the viscous oil and wear may not occur. The hydrostatic and hydrodynamic lubrications are the two typical representatives. For the hydrostatic lubrication, a pump outside should be applied to create the oil pressure and the hydrodynamic lubrication usually occurs under high speed and low load conditions [1]. A question then arises: is there a kind of lubrication mode, similar to fluid film lubrication, while the generated load carrying capacity of fluid film does not rely on any relative motions or other external facilities?

The emergence of magnetic fluid (MF) provides a new solution to this issue. MF is a colloidal dispersion of single-domain magnetic nanoparticles suspended in a carrier liquid [2]. From the lubrication point of view, MF is interesting since it can be positioned at a desired area and exhibits fluid nature. Excellent MF lubrication performance can be obtained under boundary [3], soft elasto-hydrodynamic [4] and thermal elasto-hydrodynamic [5] conditions. While for MF lubricated oil-film bearing, results show that the load-carrying capacity of the oil film can be controlled by magnetic field [6]. To achieve superior lubrication property, studies on optimizing the weight fraction of nanoparticles in MF were carried out [7,8]. Besides, the lubrication behaviors of a novel

magnetic ionic liquid and MF were compared in the case of steel/steel contacts [9]. From the bearing point of view, MF is also amusing because it can be magnetized under the action of an external magnetic field to generate an adjustable <http://yyjyc.08952.com/tgya/jfcha.asp?cha=governable&aa=4> magnetostatic force [10]. This outstanding property makes MF a very good candidate for lubrication system since the magnetostatic force can bear a load. Fig. 1a presents a copper coin floating on the surface of the magnetized MF and Fig. 1b shows the test process of confirming such force. Preliminary results indicate that the supporting force of the fluid enhances with increasing of the MF magnetization [11].

Besides the fluid support, recent works show that gas sealed by MF can also generate support [12,13]. Fig. 1c gives a MF ring attracted on the upper surface of a circular permanent magnet. On one hand, the magnetized MF ring is capable to supply fluid support ( $F_F$ , magnetostatic force). On the other hand, when the lower surface of the magnet is attached with a baseplate, the gas in the ring chamber sealed by MF is expected to afford gas support ( $F_G$ ) at the same time. As shown in Fig. 1c, according to the theoretical analysis, the gas support ( $F_G$ ) depends on the sealing capacity of the MF [12]:

$$F_G = \int_S (p_i - p_o) \cdot A_F = \mu_0 M_s (H_i - H_o) A_F \quad (1)$$

where  $p_i$  and  $p_o$  are the pressure of the inner and outer side of the MF

<sup>\*</sup> Corresponding author. Yudao street 29#, Nanjing, China  
E-mail address: [huangwei@nuaa.edu.cn](mailto:huangwei@nuaa.edu.cn) (W. Huang).

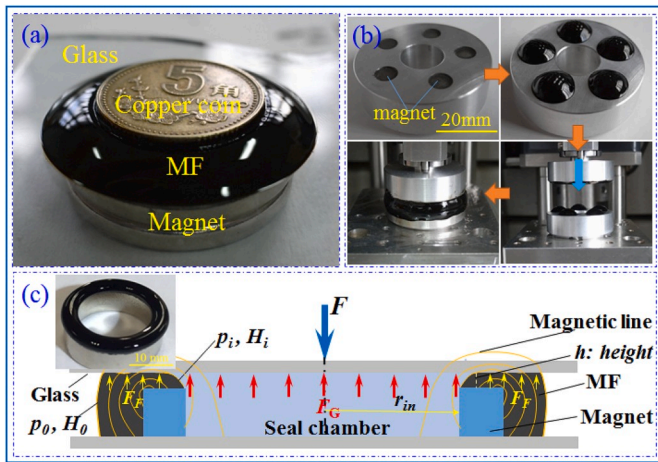


Fig. 1. (a) Copper coin supported by magnetized MF; (b) Images of the supporting force test process; (c) Schematic diagram of the support based on MF seal (The inset presents an image of an annular magnet covered with MF.).

interface,  $H_i$  and  $H_0$  are the corresponding magnetic field strength,  $\mu_0$  is the permeability of free space,  $M_s$  is the saturation magnetization of the MF and  $A_F$  ( $\pi r_{in}^2$ ) is the gas supporting area. Clearly, the introduced gas support may further enhance the total load capacity.

The analysis above shows that the bearing capacity of MF is free from any movements or pumps, and such property is highly desirable in lubrication. With the development of science and technology, device miniaturization, such as MEMS, has become a trend. Due to the high surface/volume ratio, friction and wear are crucial to performance in such systems. The advantage of MF support becomes a new avenue. However, to gain the MF support based on macro-scaled magnet (mm scale) is unrealistic and the key issue is to fabricate tiny magnet on rubbing surface. Furthermore, little is known about the effects of micro magnet structure on the MF lubrication mechanism.

Inspired by the support properties of MF absorbed on single macro-scaled magnets (see in Fig. 1, mm-scale), micro permanent magnet arrays (see in Fig. 2) were introduced to friction surfaces, forming cyclical magnetic field distribution. The load carrying capacity of MF covered on the magnet arrayed surface was investigated. Then, the lubrication performances of MF on the magnetic and normal surfaces were explored and compared. The influences of applied load and speed were taken into account. The obtained results provide a better understanding between the MF support and lubrication mechanisms based on the tiny magnet arrays.

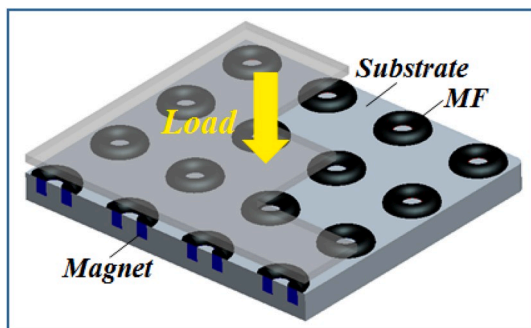


Fig. 2. Schematic diagram of micro magnet arrays for MF support and lubrication (These magnet arrays and the substrate are at the same level.).

## 2. Experimental method

### 2.1. Specimen fabrication

The micro magnet arrays are fabricated on a substrate using electrochemical machining and electroforming techniques [14]. And the main process contains four steps: photolithographic, electrochemical machining, electro-deposition and polishing. More specially, a photolithographic method was applied to prepare a photo-mask pattern with a specific geometrical shape on the substrate surface. The uncovered substrate surface was electrochemically etched in salt solution to manufacture micro-pits. Then, CoNiMnP permanent magnetic alloy with a high coercivity of 1100 Oe and remanence of 1900 Gs [15] was electro-deposited into these micro-pits. Finally, the magnet arrayed surface was polished to Ra 70 nm. After that, the micro magnet arrays were magnetized by using permanent magnets.

In this paper, two types of micro magnet arrays with round sheet and ring cells are designed and Fig. 3 shows the configuration of the arrays. These magnet arrays are fabricated on 316 stainless steel disk ( $\Phi 40$  mm  $\times$  3 mm, see in Fig. 4) and the geometric parameters of the micro magnet array on each specimen are shown in Table 1. It is estimated that about 140 micro magnets with square arrangement distribute on the disk surface. In addition, these magnet arrays and the substrate are at the same level. Fig. 4 shows the two types of final specimens and specimens absorbed with MF. As can be seen, ordered patterns of MF bulges appear on each surface due to the interaction of micro magnetic field. For comparison, specimen No.1 displays the normal surface made of 316 stainless steel disk without any micro magnets.

### 2.2. Support and friction tests

Supporting forces of MF were measured by using a custom-made setup, as described in Ref. [16] (see in Fig. 5a). Briefly, an upper plate with the size of  $\Phi 10 \times 1.0$  mm (made of 316 stainless steel) was connected with cantilever beam. During the measuring process, the micro-deformation of the beam was monitored by a laser interferometer. The force could be calculated according to the amount of deformation. The effective range and resolution of the test system were 1000 mN and 0.1 mN, respectively. The specimen absorbed with MF was placed horizontally on a mobile platform, which was right under the upper plate. As the platform shifting up with the velocity of 0.01 mm/s, the MF operating on the upper plate lead to the cantilever beam's deformation and the force was automatically recorded by a data collection system.

Two types of friction test were performed with a flat-on-flat configuration. Under the low load and speed conditions (500 mN, 0.1 mm/s), a reciprocating tribotester (Surface Measurement Machine, Sinto Scientific, Japan) was used (see in Fig. 5b) and a plate-on-disk tribotester (see in Fig. 5c) for the high load and speed conditions (2 N, 6–157 mm/s). An upper plate, the same as the supporting test used ( $\Phi 10 \times 1.0$  mm, 316 stainless steel), maintained stationary during the friction process and the lower specimen (shown in Fig. 4) was mounted on the reciprocating/rotating platform, which was connected to a motion mechanism. To sustain the upper plate aligning with the lower specimen's surface automatically, the upper plate was connected with a ball-joint holder.

Commercial MF with a saturation magnetization of 15.9 kA/m is used. It contains  $Fe_3O_4$  particles with the average size of 15 nm coated

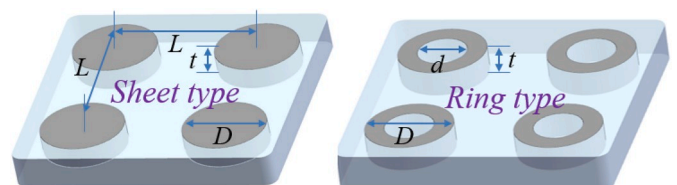


Fig. 3. Dimensional sketch of the two types of the micro magnet arrays.

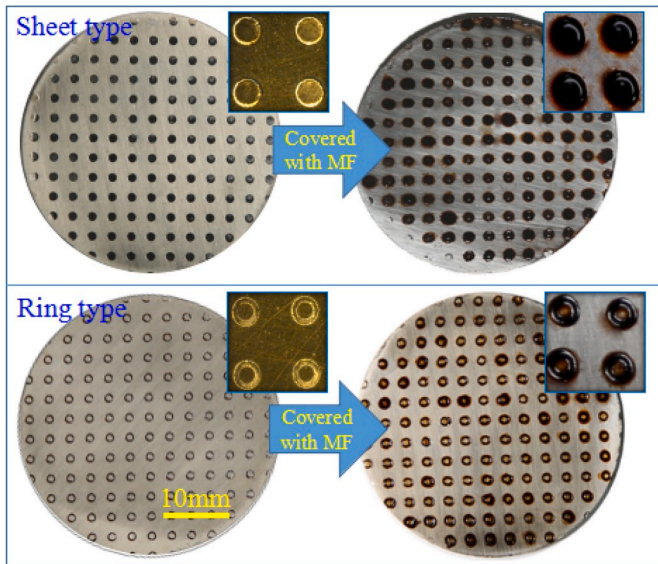


Fig. 4. Images of the final specimens covered with MF.

Table 1  
Parameters of the micro magnet array on the specimens.

| No.        | $D$ ( $\mu\text{m}$ ) | $d$ ( $\mu\text{m}$ ) | $t$ ( $\mu\text{m}$ ) | $L$ ( $\mu\text{m}$ ) |
|------------|-----------------------|-----------------------|-----------------------|-----------------------|
| 1 (normal) | 0                     | 0                     | 0                     | 0                     |
| 2 (sheet)  | 1400                  | 0                     | 80                    | 3000                  |
| 3 (ring)   | 1400                  | 800                   | 40                    | 3000                  |
| 4 (ring)   | 1400                  | 800                   | 80                    | 3000                  |
| 5 (ring)   | 1400                  | 800                   | 120                   | 3000                  |

by a lay of oleic acid as surfactant. The carrier liquid is diester with the viscosity of 50 mPa s, which is lower than that of the MF (79 mPa s). For each support and friction tests, the dosage of 0.5 mL MF is dropped on the lower specimen's surface.

During the experiments, the five specimens in Table 1 are divided in two groups. To explore the effects of magnet arrays (including shapes) on MF support and lubrication behaviors, three specimens (No.1, 2 and 4) are in one group. And ring typed specimens (No.3, 4 and 5) are in the other group to figure out the thickness influence of the micro magnets. Each of the test was repeated three times for the 5 specimens.

### 3. Results and discussion

Fig. 6 shows the supporting capacity of MF covered on the normal (No.1) and magnetic (No.2–5) surfaces. As the specimen approaches to the upper plate, the normal surface shows a negligible supporting force and the trivial force may come from the viscosity resistance of MF. While on the magnetic surfaces, the forces increase obviously and the values enhance gradually as the specimen moves up. It is known that MF is an assembly of superparamagnetic nanoparticles in a carrier liquid and the dipole moment of each particle is oriented randomly in the zero field case. However, in an applied magnetic field, the particle moment will arrange along the orientation of the field, exhibiting macroscopic magnetization. The magnetization of the MF may induce attractive force on each particle, which will transform to the bulk fluid as a body force [17]. And during the bearing process, the body force manifests itself an ability of static fluid support ( $F_F$ ), shown in Fig. 1. Usually, the attractive force increases proportionally to the applied magnetic field strength [10]. As the distance between the specimen and the upper plate decreasing, the strength of the field forced on the MF enhances gradually. Consequently, attraction between individual particles reinforces, resulting in the macroscopic increment of the supporting force.

Furthermore, as can be seen in Fig. 6a, the supporting force

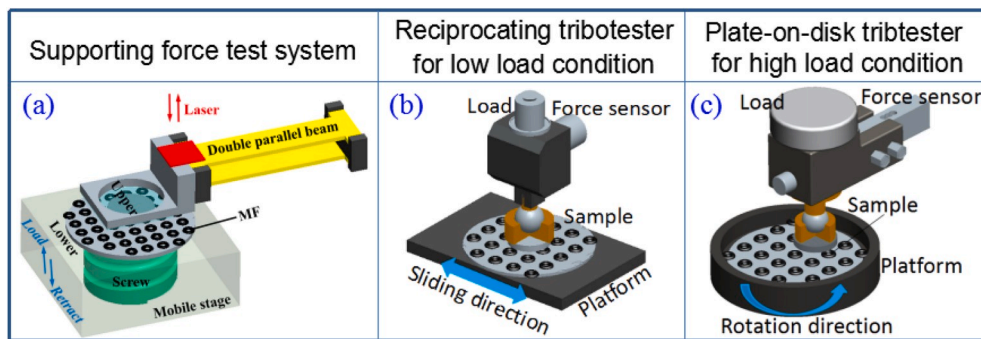


Fig. 5. Schematic diagrams of the supporting and friction test systems.

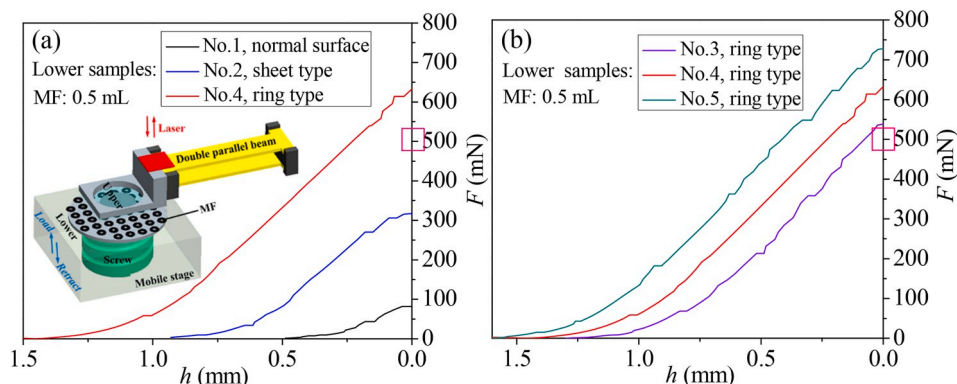


Fig. 6. Dependence of the supporting forces on the height ( $h$ ) between the lower specimen and the upper plate.

generated on the surface with micro ring cell (No.4) is almost twice higher than that of the specimen with sheet cell (No.2). In addition, the force produced on the ring type specimens also rises with the increment of the magnet thickness (see in Fig. 6b). To explain the phenomena, the magnetic field distribution on the four surfaces (No.2–5) was calculated by using a software of Ansoft Maxwell 3D model. The magnetic and geometrical parameters input were in accordance with each specimen and the results are given in Fig. 7 (height: 0.3 mm). It seems that the maximum strength of the field is concentrated at the edge of each magnet cell. For the sheet type specimen (No.2), the supporting force only origins from the magnetized MF, and it is a kind of fluid support ( $F_F$ ), which is directly related with external field strength. For the ring type specimen, besides the fluid support, the gas sealed by MF in each micro cavity may create an extra supporting force ( $F_G$ ). As can be seen in Fig. 7a and c, due to the same magnitude of the field strength between specimens No.2 and No.4 ( $6 \times 10^3$  A/m), the ring type specimen exhibits the higher support capacity.

While for the three ring type specimens, the supporting behavior is more or less the same (see in Fig. 6b). Since the demagnetizing factor of magnet declines with the increment of axial dimension [15], the surface magnetic strengths increase steadily with the increasing of micro magnet thickness. Such results were confirmed by the magnetic field simulation (see in Fig. 7b, c and d). The enhanced field strength will not only benefit the fluid support improvement, but also promote the MF seal capacity on each micro magnet cell according to the MF sealing principle [18]. As shown in Fig. 1c, with the decrease of the height ( $h$ ), the inner interface of MF moves to the position with higher magnetic field strength ( $H_i$ ) while the outer shifts to the lower one ( $H_o$ ). Based on Eq. (1), the gas support ( $F_G$ ) will increase gradually due to the increased ( $H_i - H_o$ ). Hence, the total bearing force tested on the ring type specimens grows with the increasing micro magnet thickness.

Fig. 8 shows the friction curves versus time of the five specimens under the low load of 500 mN, which is chosen based on the results of supporting tests (see in Fig. 6). As shown in Fig. 8a, the normal surface (No.1) expresses the highest friction coefficient in general. The value decreases from 0.13 at the beginning and stabilizes at 0.08. As expected, the coefficients decline obviously for the magnetic surfaces. Due to the

normal load applied has surpassed the ultimate support capacity of specimen No.2 (320 mN), it can be deduced that the load is shared by the MF support and asperity contacts together. The stable coefficient value is about 0.03, corresponding to the mixed lubrication state. The lowest friction coefficient of 0.003 appears for the ring type specimen No.4. Since its ultimate load (630 mN) is higher than the applied load, it means the tribo-pairs can be fully isolated by the MF film and squeezed gas in the MF seal unit. Thus, friction force is only associated with the internal shearing of the MF.

The low frictions are further confirmed when using the three ring type specimens (see in Fig. 8b). Note that the coefficient of specimen No.3 is a litter higher than the other two, and the reason may also be related with its lower support capacity (see in Fig. 6b). When the bearing force is much larger than the normal load, low friction coefficient of 0.003 regains. To figure out the superiority of MF lubrication on the micro magnet arrayed surface, three other lubricants (silicone oil, PAO and diester) were used and the results were presented in Fig. 8c. Compared with conventional lubricants, due to the support capacity, the tribo-pairs are separated by the supporting force and the MF on the magnetic surface presents the lowest friction coefficient.

It shows that as long as the mass of an object is less than the capacity of the MF supporting system, it will float on the surface of MF. Moreover, unlike the classic hydrodynamic or hydrostatic lubrications, such MF bearing structure does not rely on relative motion or pumps and it can provide bearing force in the stationary state. Such result could greatly relieve the “stick-slip” behavior in the precise and low speed mechanisms.

Besides the low load condition, lubrication behaviors under a high load were also conducted with a series of sliding speeds from 0.006 to 0.157 m/s. Fig. 9 shows the stable original friction curves of the two specimens (No.1 and No.4) at the sliding speed of 0.157 m/s, where the magnet arrayed specimen presents obvious friction reduction. To estimate the general effects of the magnet arrays, specimens at each speed were performed for 300 s and the stable data of the last 60 s was averaged as the final result. Fig. 10 summarizes the frictional transition of each specimen lubricated with MF in Stribeck curve format. During this procedure, the lubricant film is very thin at low speed condition and film

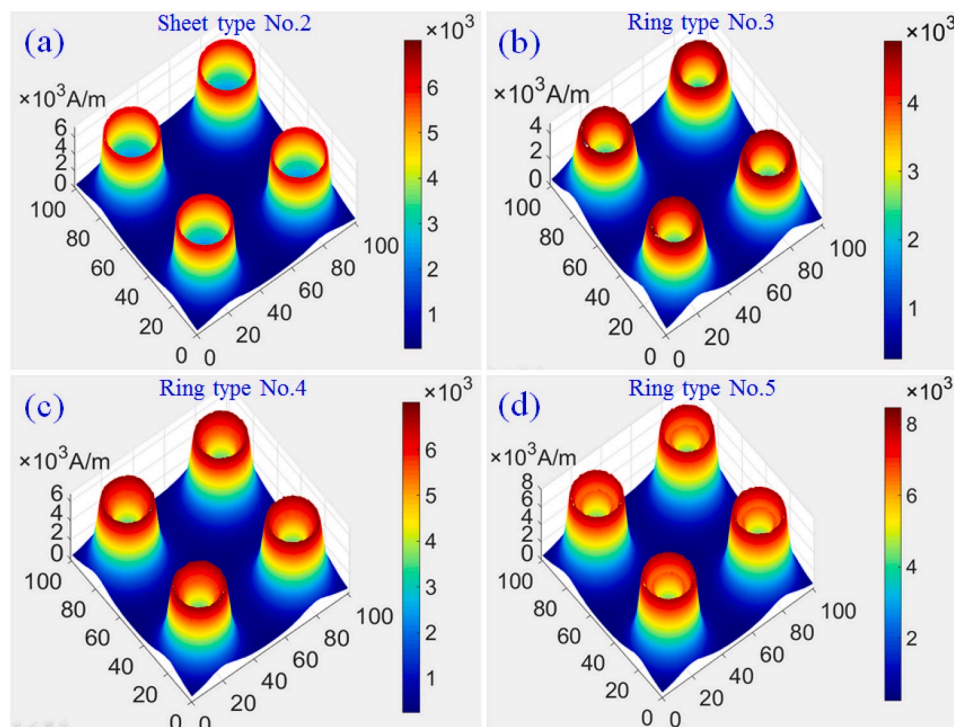


Fig. 7. 3D-visualization of magnetic field distribution on each surface.

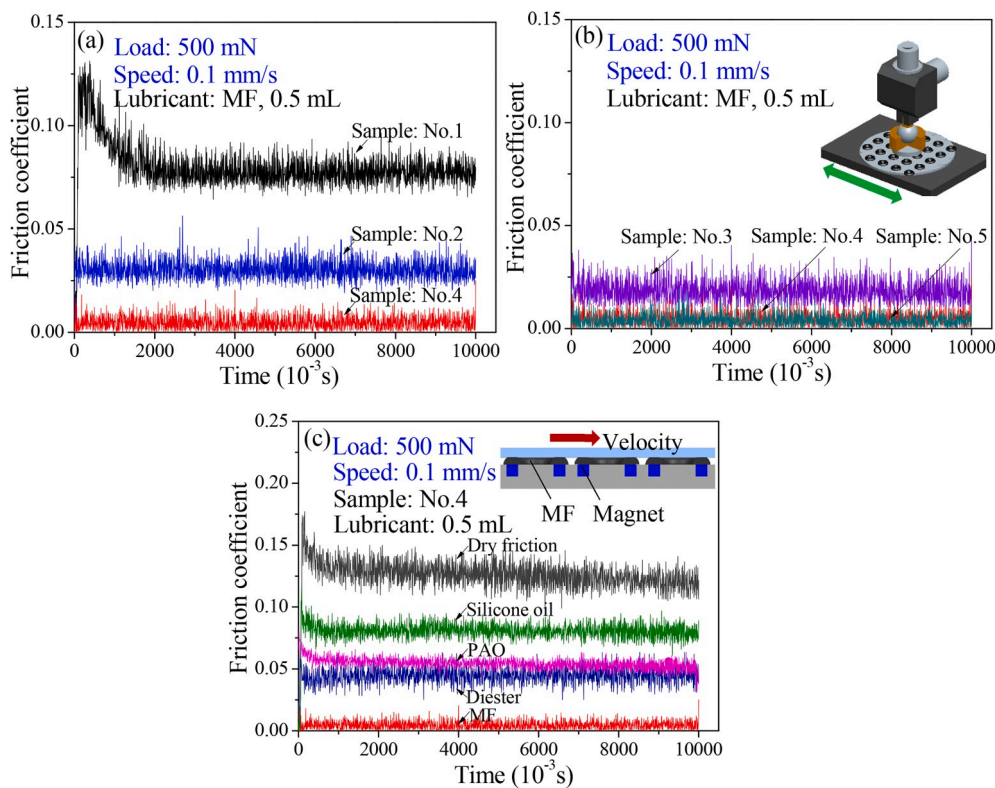


Fig. 8. Friction curves of the five samples lubricated with MF at low load and speed conditions (a) and (b); Friction curves of sample No.4 lubricated with different lubricants (c).

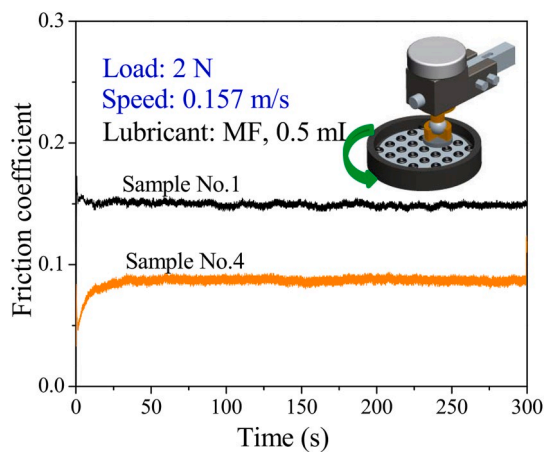


Fig. 9. Friction curves of the samples (No.1 and No.4) under a high load of 2 N.

thickness changes with the increase of the speed, leading to the transitions of contact and lubrication state [19]. The indications of the lubrication regime can be estimated according to the friction coefficients.

Fig. 10 summarizes the influence of micro magnet arrays on transition in lubrication regimes. Obvious differences appear between the normal and magnetic surfaces in Fig. 10a. For the normal surface (No.1), the coefficients of friction rise with the increment of the sliding speed with no transitions. Based on the Stribeck curve [20], even at a low speed condition, the tribo-pairs can get into the full film lubrication. While for the magnet arrayed specimens (No.2 and No.4), the coefficients changes from a high value of about 0.05 at the speed of 0.006 m/s to a lower value of 0.03 as the speed increases to 0.019 m/s. After that, the coefficients of friction grow continuously as the speed elevates. Such

occurrences indicate that, the formation of full MF film is capable to separate and lubricate the tribo-pairs, and the frictional state on the magnetic surfaces transforms from the mixed to the hydrodynamic lubrication regimes. In comparison to the normal surface, the surface with micro magnet cells presents a friction increment at the low speed condition. The main reason can be attributed to the presence of magnetic field. Due to the absorption of the micro magnets, the fluid spreading can be restrained partly [21] and uniform MF film cannot be formed on the rubbing surface. Moreover, magnetic particles suspended in carried liquid will line up with the magnetic field, resulting in viscosity increment [22], which will also enhance the friction force. On the contrary, MF may flow smoothly on the surface of specimen No.1 and form effective lubricant film even at a very low speed condition.

It is interesting to find that the magnetic surfaces (No.2 and No.4) present friction reduction at high speed condition compared with the normal surface (Fig. 10a). In the absence of magnetic field, MF is similar as the conventional lubricant. Caused by the centrifugation, parts of the MF spatters away from the rubbing surface. While due to the micro magnet arrays, more MF is absorbed on the surface as lubricant, which could be the dominate reason for friction reduction. Besides, because of the effect of shear thinning [3], the viscosity of MF decreases at the higher shear rates, which is also conducive to reducing friction in the hydrodynamic lubrication state [23].

As observed in Fig. 10b, the specimen with thicker micro magnet shows better lubrication property, especially at the higher speed conditions. Usually, the magnetization of the MF is the function of the applied magnetic field at isothermal condition. Thus, the induced magnetic force  $f_m$  of MF can be represented as [24]:

$$f_m = \mu_0 X_m H \cdot \nabla H \quad (2)$$

where  $\mu_0$  is the permeability of free space,  $X_m$  is the magnetic susceptibility of MF,  $H$  and  $\nabla H$  are the applied magnetic field strength and gradient.

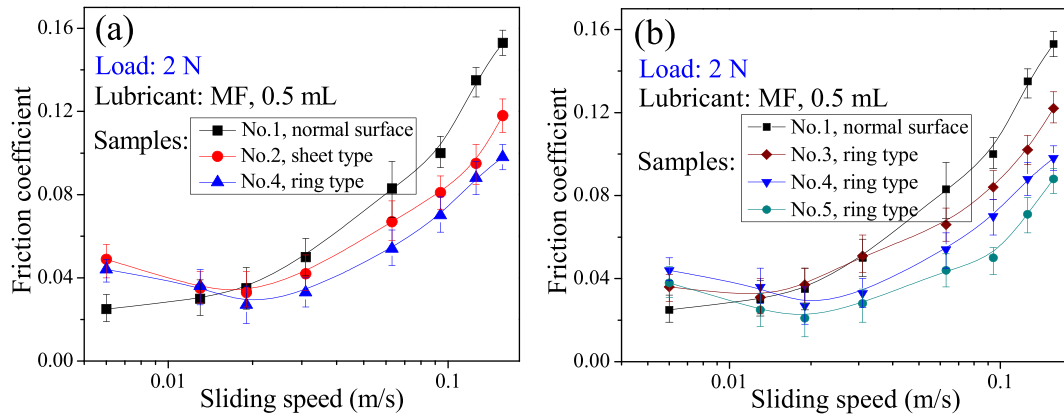


Fig. 10. Summary of the MF lubrication in Stribeck curve format.

Based on Eq. (2), the interaction force between the micro magnet and MF grows with the increment of surface field strength. Due to enlarged magnetic strength, the centrifugal effect may be inhibited dramatically and more MF can be remained on the sliding surface, forming effective lubrication film. Besides, as mentioned in Refs. [23,25], the higher magnetic field strength would help boost the load carrying capacity of the MF lubrication film. Therefore, specimen No.5 presents the best friction behaviors and its coefficient of friction declines by 27.8% compared with that of the specimen No.3 at the speed of 0.157 m/s.

Fig. 11 presents a summary of the coefficient differences between magnetic and normal specimens under the load of 2 N. In general, magnetic surfaces lubricated with MF show friction increment at the low speed conditions. As the speed is over 0.013 m/s, all the magnetic specimens exhibit an anti-friction property. The higher speed it is, the greater the difference is. Meanwhile, as the thickness of the micro magnets expands, the anti-friction performance becomes more obvious.

#### 4. Conclusions

To achieve static support of MF, two types of micro magnet (sheet and ring) arrays were introduced to friction surfaces, forming cyclical magnetic field distribution. The support and lubrication behaviors of MF on the two surfaces were tested and compared. According to the results presented, the following main conclusions can be drawn.

- (1) The supporting capacity of MF absorbed on micro magnet arrays was confirmed. Compared with the sheet typed surface, MF on the ring typed micro magnets can generate the higher supporting force. And the force increases with the increasing thickness of the magnet cell.
- (2) Under the low load condition (500 mN), as the force supplied by the MF supporting structure is much larger than the normal load, low friction coefficient of 0.003 can be achieved.
- (3) Under the high load condition (2 N), the magnetic surfaces lubricated with MF only show friction reduction at the higher speeds. Additionally, as the thickness of the micro magnet cell increases, the anti-friction behavior becomes more evident.

#### Declaration of competing interest

The authors declare that they have no known competing financial interests or personal relationships that could have appeared to influence the work reported in this paper.

#### CRediT authorship contribution statement

Jingbing Li: Writing - original draft. Qingwen Dai: Visualization, Investigation. Wei Huang: Conceptualization, Writing - review &

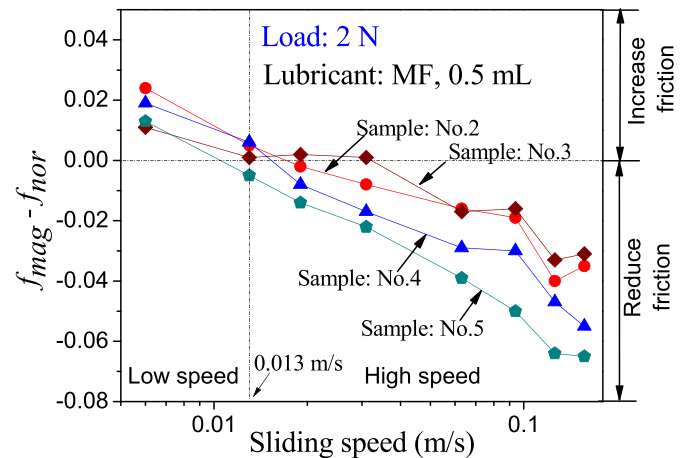


Fig. 11. Summary of the coefficient difference between magnetic and normal surfaces ( $f_{mag}$  and  $f_{nor}$  are the friction coefficients of magnetic and normal surfaces shown in Fig. 10).

editing. Xiaolei Wang: Supervision.

#### Acknowledgements

The authors thank the National Natural Science Foundation of China (No.51875278) for financial support.

#### References

- [1] Boyde S. Green lubricants. *Environmental benefits and impacts of lubrication*. The Royal Society of Chemistry 2002;4:293–307.
- [2] Scherer C, Neto AMF. Ferrofluids: properties and applications. *Braz J Phys* 2005; 35:718–28.
- [3] Uhlmann E, Spur G, Bayat N, Patzward R. Application of magnetic fluids in tribotechnical systems. *J Magn Magn Mater* 2002;252:336–40.
- [4] Andablo-Reyes E, de Vicente J, Hidalgo-Álvarez R, Myant C, Reddyhoff T, Spikes HA. Soft elasto-hydrodynamic lubrication. *Tribol Lett* 2010;39:109–14.
- [5] Zhao J, Wang Y, Zhang P, Jian G. A Newtonian thermal elastohydrodynamic lubrication model for ferrofluid-lubricated involute spur gear pair. *Lubric Sci* 2020; 32:33–45.
- [6] Wang J, Kang J, Zhang Y, Huang X. Viscosity monitoring and control on oil-film bearing lubrication with ferrofluids. *Tribol Int* 2014;75:61–8.
- [7] Trivedi K, Parekh K, Upadhyay RV. Nanolubricant: magnetic nanoparticle based. *Mater Res Express* 2017;4:114003.
- [8] Wang L, Guo C, Ryuichiro Y. Experimental research on tribological properties of  $Mn_{0.78}Zn_{0.22}Fe_2O_4$  magnetic fluids. *J Tribol* 2008;130:031801.
- [9] Jia J, Yang G, Zhang C, Zhang S, Zhang Y, Zhang P. Effects of magnetic ionic liquid as a lubricant on the friction and wear behavior of a steel-steel sliding contact under elevated temperatures. *Friction* 2019. <https://doi.org/10.1007/s40544-019-0324-0>.
- [10] Rosensweig RE. *Ferrohydrodynamics*. Cambridge University Press; 1985.

- [11] Huang W, Shen C, Wang X. Study on static supporting capacity and tribological performance of ferrofluids. *Tribol Trans* 2009;52:717–23.
- [12] Wang Z, Hu Z, Huang W, Wang X. Elastic support of magnetic fluids bearing. *J Phys Appl Phys* 2017;50:435004.
- [13] Lampaert SGE, Spronck JW, van Ostayen RAJ. Load and stiffness of a planar ferrofluid pocket bearing. *Proc IME J J Eng Tribol* 2017;232:14–25.
- [14] Shen C, Huang W, Ma G, Wang X. A novel surface texture for magnetic fluid lubrication. *Surf Coating Technol* 2009;204:433–9.
- [15] Cho HJ, Bhansali S, Ahn CH. Electroplated thick permanent magnet arrays with controlled direction of magnetization for MEMS application. *J Appl Phys* 2000;87:6340–3.
- [16] Li M, Huang W, Wang X. Advanced adhesion and friction measurement system. *Meas Sci Technol* 2017;28:035601.
- [17] Oldenburg C, Borglin SE, Moridis GJ. Numerical simulation of ferrofluid flow for subsurface environmental engineering applications. *Transport Porous Media* 2000;38:319–44.
- [18] Li D, Xu H, He X, Lan H. Study on the magnetic fluid sealing for dry Roots pump. *J Magn Magn Mater* 2005;289:419–22.
- [19] Kovalchenko A, Ajayi O, Erdemir A, Fenske G, Etsion I. The effect of laser surface texturing on transitions in lubrication regimes during unidirectional sliding contact. *Tribol Int* 2005;38:219–25.
- [20] Nakano M, Miyake K, Korenaga A, Sasaki S, Ando Y. Tribological properties of patterned NiFe-covered Si surfaces. *Tribol Lett* 2009;35:133–9.
- [21] Ke H, Huang W, Wang X. Controlling lubricant migration using ferrofluids. *Tribol Int* 2016;93:318–23.
- [22] Odenbach S. Ferrofluids—magnetically controlled suspensions. *Colloid Surface Physicochem Eng Aspect* 2003;217:171–8.
- [23] Shahrivar K, de Vicente J. Ferrofluid lubrication of compliant polymeric contacts: effect of non-homogeneous magnetic fields. *Tribol Lett* 2014;56:281–92.
- [24] Nada GS, Osman TA. Static performance of finite hydrodynamic journal bearings lubricated by magnetic fluids with couple stresses. *Tribol Lett* 2007;27:261–8.
- [25] Shukla JB, Kumar D. A theory for ferromagnetic lubrication. *J Magn Magn Mater* 1987;65:375–8.